1   **Short Title:** *DCLs* **and siRNAs in Intra- and Intercellular VIGS**

2

3   **Corresponding Author:** Yiguo Hong

4   Research Centre for Plant RNA Signaling, College of Life and Environmental Sciences,

5   Hangzhou Normal University, Hangzhou 310036, China and Warwick-Hangzhou RNA

6   Signaling Joint Laboratory, School of Life Sciences, University of Warwick, Coventry

7   CV4 7AL, UK.

8

9   **Telephone:**   +86-571-28866065

10   **Fax:**   +86-571-28866065

11   **E-mails:**   yiguo.hong@hznu.edu.cn; yiguo.hong@warwick.ac.uk

12

13   **Primary Research Area:** Virus-plant interactions/Cell Biology

14   **2nd Research Area:** Cell- and non-cell autonomous VIGS/Signaling and Response

Roles of Dicer-Like proteins 2 and 4 in Intra- and Intercellular Antiviral Silencing[1]

Cheng Qin[2], Bin Li[2], Yaya Fan[2], Xian Zhang[2], Zhiming Yu[2], Eugene Ryabov, Mei Zhao, Hui Wang, Nongnong Shi, Pengcheng Zhang, Stephen Jackson, Mahmut Tör, Qi Cheng, Yule Liu, Philippe Gallusci, and Yiguo Hong[*]

Research Centre for Plant RNA Signaling, College of Life and Environmental Sciences, Hangzhou Normal University, Hangzhou 310036, China (C.Q., B.L., Y.F., X.Z., Z.Y., E.R., M.Z., H.W., N.S., P.C., Y.H.); Warwick-Hangzhou RNA Signalling Joint Laboratory, School of Life Sciences, University of Warwick, Warwick CV4 7AL, UK (E.R., S.J., Y.H.); Institute of Science and the Environment, University of Worcester, Worcester WR2 6AJ, UK (M.T.); Biotechnology Research Institute, Chinese Academy of Agricultural Sciences, Beijing 100081, China (Q.C.); MOE Key Laboratory of Bioinformatics, Centre for Plant Biology, School of Life Sciences, Tsinghua University, Beijing 100084, China (Y.L.); l'UMR Ecophysiologie et Génomique Fonctionnelle de la Vigne, ISVV, 210 Chemin de Leysotte, CS 50008, 33882 Villenave d'Ornon, France (P.G.).

[2]These authors contributed equally to this work.

45   **Author Contributions:** C.Q., B.L., Y.F., X.Z., and Z.Y. designed, performed

46   experiments and analysed data; E.R. performed bioinformatics analysis. M.Z., H.W., N.S.

47   and P.Z. performed research; S.J., M.T., Y.L. and Q.C. were involved in the analysis of

48   data and helped writing the paper. Y.H. conceived and initiated the project, designed

49   experiments, analysed data and wrote the paper.

50

51   **One-sentence Summary:** DCL4 inhibited intercellular VIGS whilst DCL2 along with DCL2-

52   processed/dependent siRNAs were involved in non-cell autonomous VIRS in Nicotiana benthamiana.

53

54   [*]Address correspondence to yiguo.hong@hznu.edu.cn; yiguo.hong@warwick.ac.uk

55   The author responsible for distribution of materials integral to the findings presented in

56   this article in accordance with the policy described in the instructions for Authors

57   (www.plantphysioll.org) is: Yiguo Hong (yiguo.hong@hznu.edu.cn,

58   yiguo.hong@warwick.ac.uk).

ABSTRACT

59   **ABSTRACT**

60   RNA silencing is an innate antiviral mechanism conserved in organisms across kingdoms.

61   Such a cellular defence involves DICER or DICER-LIKEs (DCLs) that process plant

62   virus RNAs into viral small interfering (vsi)RNAs. Plants encode four *DCLs* which play

63   diverse roles in cell-autonomous intracellular virus-induced RNA silencing (known as

64   VIGS) against viral invasion. VIGS can spread between cells. However, the genetic basis

65   and involvement of vsiRNAs in non-cell autonomous intercellular VIGS remains poorly

66   understood. Using GFP as a reporter gene together with a suite of *DCL* RNAi transgenic

67   lines, here we show that despite the well-established activities of *DCLs* in intracellular

68   VIGS and vsiRNA biogenesis, *DCL4* acts to inhibit intercellular VIGS whilst *DCL2* is

69   required (likely along with DCL2-processed/dependent vsiRNAs and their precursor

70   RNAs) for efficient intercellular VIGS trafficking from epidermal to adjacent cells.

71   *DCL4* imposed an epistatic effect on *DCL2* to impede cell-to-cell spread of VIGS. Our

72   results reveal previously unknown functions for *DCL2* and *DCL4* which may form a dual

73   defensive frontline for intra- and intercellular silencing to double-protect cells from virus

74   infection in *Nicotiana benthamiana*.

75

76   **Keywords:** DICER-LIKEs, vsiRNAs, non-cell autonomous intercellular VIGS,

77   *Nicotiana benthamiana*

INTRODUCTION

RNA silencing targets endogenous cellular nucleic acids and exogenous invasive pathogenic RNAs or DNAs for homologous RNA-dependent degradation, translation repression or RNA-directed DNA methylation (RdDM) in eukaryotic organisms (Baulcombe, 2004; Sarkies and Miska, 2014). In plants, RNA silencing forms an innate defence against virus infection (Aliyari and Ding, 2009; Csorba et al., 2015). Such an antiviral mechanism involves DICER-LIKE (DCL) ribonuclease type III enzymes. Most plants encode four DCLs of which DCL1 is responsible for production of microRNA whilst DCL2, DCL3 and DCL4 are responsible for biogenesis of 22, 24 and 21nt small interfering RNA (siRNA), respectively (Mukherjee et al., 2013). DCL2 and DCL4 possess partially redundant functions in the production of trans-acting siRNA, but DCL2 acts predominantly to manufacture various sized secondary siRNAs (Chen et al., 2010; Henderson et al., 2006; Xie et al., 2005). Unlike animal viruses, plant viruses have not yet been found to encode any microRNA or specific site that can be targeted by host cellular microRNAs. However, artificial microRNAs can inhibit plant virus invasion (Qu et al., 2007). In *Arabidopsis*, DCLs can process plant virus RNAs into vsiRNAs within individual cells. For instance, *DCL4* and DCL4-processed 21nt vsiRNAs are involved in virus-induced RNA silencing (also known as VIGS), a kind of post-transcriptional gene silencing (PTGS; Bouche et al., 2006; Garcia-Ruiz et al., 2010; Qu et al., 2008). *DCL2* and its cognate 22nt vsiRNAs may also affect VIGS in plant cells when *DCL4* is absent or defective (Andika et al., 2015; Wang et al., 2011; Zhang et al., 2012). On the other hand, *DCL3* and 24nt vsiRNAs are associated with RdDM and transcriptional gene silencing (TGS) in the protection of plant cells from DNA virus infection (Aregger et al., 2012; Blevins et al., 2006). In *Arabidopsis*, *DCL4* and *DCL2* also play hierarchical and redundant roles in intracellular antiviral silencing (Bouche et al., 2006; Garcia-Ruiz et al., 2010; Wang et al., 2011). Recently, a combined activity of *DCL2* and *DCL3* has been reported to be critical in defending plants from viroid infection (Katsarou et al., 2016). DCL1 can negatively regulate DCL4-initiated antiviral RNA silencing pathway (Qu et al., 2008). However, the roles of the different *DCLs* in promoting intercellular VIGS for plant systemic acquired resistance to virus infection are unclear.

5

108   In response to virus infection, intracellular VIGS in the initial virus-infected cells

109   triggers intercellular silencing in adjacent cells, which spreads systemically to remote

110   tissues. This is known as non-cell autonomous VIGS. Non-cell autonomous VIGS

111   combats incoming viruses and protects recipient cells from further viral invasion

112   (Schwach et al., 2005). In *Arabidopsis*, spread of the phloem-originating PTGS from

113   companion cells to nearby cells requires *DCL4* and DCL4-processed 21nt siRNA signals

114   (Dunoyer et al., 2005). However, whether 21nt siRNAs represent the bona fide silencing

115   signals that are transportable among plant cells is highly controversial (Berg, 2016). On

116   the other hand, *DCL2* can stimulate transitive PTGS and biogenesis of secondary siRNAs

117   (Mlotshwa et al., 2008). *DCL2* can also restore silencing in the *Arabidopsis dcl4* mutant

118   that is deficient in cell-to-cell spread of transgene-mediated PTGS (Parent et al., 2015).

119   Moreover, intercellular and systemic PTGS involve many cellular factors including

120   RDR6 which has been shown to be required for efficient cell-to-cell movement of VIGS

121   (Melnyk et al., 2011; Qin et al., 2012; Searle et al., 2010; Smith et al., 2007).

122   Nonetheless, the genetic basis and requirement of vsiRNAs for cell-to-cell and systemic

123   spread of antiviral VIGS remain to be elucidated.

124   We previously developed a Turnip crinkle virus (TCV)-based local silencing

125   assay to investigate intra- and intercellular VIGS in *Nicotiana benthamiana* (Qin et al.,

126   2012; Ryabov et al., 2004; Shi et al., 2009; Zhou et al., 2008). TCV belongs to

127   *Carmovirus* with a single positive-stranded RNA genome (Carrington et al., 1989). It

128   encodes five proteins, namely the RNA-dependent RNA polymerases P28 and its read-

129   through P88, movement proteins P8 and P9 and coat protein (CP) P38 (Carrington et al.,

130   1989; Hacker et al., 1992; Li et al., 1998). CP is a strong <u>v</u>iral <u>s</u>uppressor of <u>R</u>NA

131   silencing (VSR; Chattopadhyay et al., 2015; Merai et al., 2006; Perez-Canamas et al.,

132   2015; Qu et al., 2003; Thomas et al., 2003; Zhang et al., 2012). It is also required for cell-

133   to-cell movement of TCV in *N. benthamiana* (Cohen et al., 2000; Li et al., 2009).

134   TCV/GFPΔCP in which CP is replaced with the 714nt GFP sequence (dubbed *TcvGFP*

135   hereafter) is movement-deficient. This movement-deficient virus is still infectious but the

136   virus remains restricted to the infected cell (Ryabov et al., 2004). Cell-to-cell spread of

137   TCV/GFPΔCP can be complemented by heterologous silencing suppressors (Shi et al.,

138   2009). However in the absence of the strong VSR CP, the movement-deficient

6

139 TCV/GFPΔCP can initiate intracellular VIGS that efficiently spreads to neighbouring

140 epidermal and mesophyll cells (Qin et al., 2012; Ryabov et al., 2004; Shi et al., 2009;

141 Zhou et al., 2008). Using this intra- and intercellular VIGS assay together with a suite of

142 transgenic *DCL* RNAi lines, we have examined how the different *DCLs* affect viral

143 siRNA biogenesis, intra- and intercellular VIGS in *N. benthamiana*. Our findings lead us

144 to propose a model where intra- and intercellular VIGS comprise two separate

145 components of an integrated viral defence strategy in which *DCL2* and *DCL4* play

146 different roles.

147

148

7

149 **RESULTS**

150 ***DCL* RNAi Does Not Affect Cell-to-Cell Mobility of TCV/GFPΔCP**

151 To dissect the genetic requirements and silencing signals involved in non-cell

152 autonomous intercellular VIGS (Fig. 1) in *N. benthamiana* (*Nb*), we utilized a suite of

153 *DCL* RNAi transgenic *Nb* lines including *DCL1i*; *DCL2Ai* and *DCL2Bi*; *DCL3Ai* and

154 *DCL3Bi*; *DCL4Ai* and *DCL4Bi*; and one double RNAi line *DCL24i* (Supplemental Table

155 S1). We also used *GFP* transgenic lines *16cGFP*; *GfpDCL1i*; and lines *Gfp*; *GfpDCL2Ai*

156 and *GfpDCL2Bi*; *GfpDCL3Ai* and *GfpDCL3Bi*; *GfpDCL4Ai* and *GfpDCL4Bi*, which were

157 derived from crosses between *16cGFP* and *Nb* or *DCL* RNAi lines, respectively, as well

158 as a triple cross line *GfpDCL24i* (Supplemental Table S1). We performed qRT-PCR

159 assays and revealed that *DCL2, DCL3* and *DCL4* transcript levels were down-regulated

160 by 60-80% in each of the two independent RNAi lines; however only about 40%

161 reduction was achieved for *DCL1* in *DCL1i* (Fig. 1A). We then analyzed the impact of

162 *DCL* RNAi on cell-to-cell mobility of TCV/GFPΔCP (Fig. 1B-G). The upper epidermises

163 of leaves in each *DCL* RNAi plant at the six-leaf stage were inoculated with

164 TCV/GFPΔCP. As observed under the fluorescent microscope, strong GFP green

165 fluorescence appeared only in single epidermal cells in leaves of the wild-type *Nb* control

166 (Fig. 1C) and all *DCL* RNAi plants (Fig. 1D-G). These results demonstrate that presence

167 of TCV/GFPΔCP was limited to individual virus-infected epidermal cell, and that *DCL*

168 RNAi did not affect the movement-deficiency of TCV/GFPΔCP.

169

170 ***DCL4* RNAi Enhances, whilst *DCL2* RNAi Reduces, Cell-to-Cell Spread of VIGS**

171 To test whether intra- and intercellular VIGS is affected by the down-regulation of

172 individual *DCL* genes, we used GFP as a reporter and mechanically inoculated the

173 movement-deficient TCV/GFPΔCP onto young leaves of *16cGFP* (Fig. 1H), *GfpDCL1i*

174 (Fig. 1I), *Gfp* (Fig. 1J), *GfpDCL2Ai* and *GfpDCL2Bi* (Fig. 1K and L), *GfpDCL3Ai* and

175 *GfpDCL3Bi* (Fig. 1M and N) and *GfpDCL4Ai* and *GfpDCL4Bi* (Fig. 1O and P) plants.

176 We then counted the number of *GFP* silencing foci on both upper and lower epidermises

177 of the inoculated leaves, and measured sizes in diameter of 80-560 randomly selected

178 silencing foci on the upper epidermises (Fig. 1H-U; Supplemental Table S2). We used

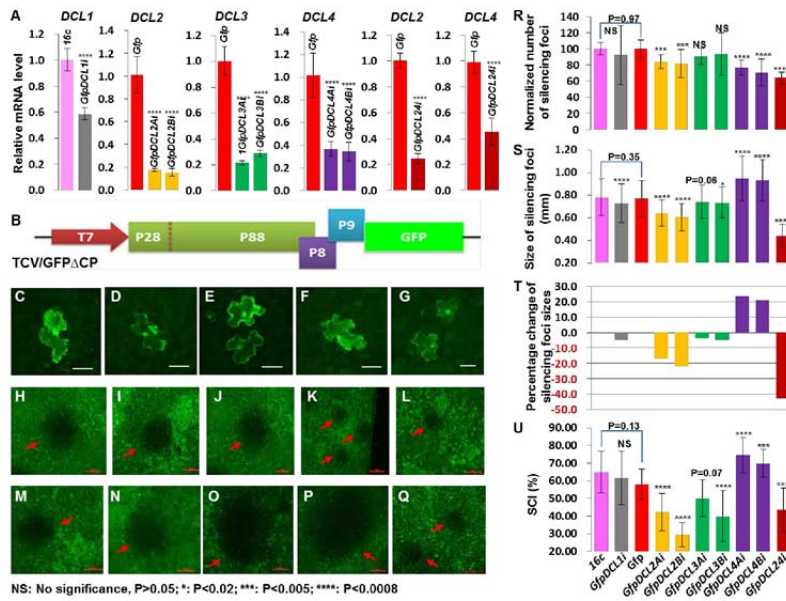179 the number and size of silencing foci as well as the 'silencing cell-to-cell-spread index

Figure 1. Different Roles of *DCLs* in the Cell-to-cell Spread of VIGS. (A) Down-regulation of *DCL* expression by RNAi. Young leaves were collected from *DCLi* plants at 7 days post-inoculation (dpi), and the level of *DCL* RNAs was analysed by qRT-PCR. (B) Schematic of the intracellular RNA silencing trigger TCV/GFPΔCP. The T7 promoter, viral RNA-dependent RNA polymerases (P28, P88), movement proteins (P8 and P9) and GFP are indicated. (C-G) Restricted localization of TCV/GFPΔCP in single epidermal cell of *Nb* (C), *DCL1i* (D) *DCL2Ai* (E), *DCL3Bi* (F) and *DCL4Ai* (G) plants. (H-Q) Intercellular *GFP* silencing foci (dark patches indicated by red arrows). Photographs of silencing foci on leaves of *16cGFP* (H); *GfpDCL1i* (I); *Gfp* (J); *GfpDCL2Ai* (K) and *GfpDCL2Bi* (L); *GFPDCL3Ai* (M) and *GfpDCL3Bi* (N); *GfpDCL4Ai* (O) and *GfpDCL4Bi* (P); and a triple-cross line *GfpDCL24i* (Q), were taken under a fluorescent microscope at 7 dpi. Bar=500μm. (R) Normalized number of *GFP* silencing foci per upper epidermis. Silencing foci were counted at 7 dpi from 3-21 different plant leaves inoculated with TCV/GFPΔCP. (S) and (T) Average size (diameters, S) and percentage change (T) of silencing foci. 80-560 silencing foci on different upper epidermises were randomly selected and measured. (U) SCI calculated as percentage of number of silencing foci on lower epidermis out of the number of silencing foci on upper epidermis. Student's *t*-tests were performed for qRT-PCR and silencing data (mean ± standard deviation) and P-values are indicated (asterisks).

180   (dubbed SCI hereafter)' to assess the influence of *DCL* RNAi on intra- and intercellular

181   VIGS (Supplemental Text S1). Compared to *16cGFP* and *Gfp* controls (Fig. 1H and J),

182   *DCL2* RNAi caused 17-22% decrease in the average sizes of silencing foci (Fig. 1K, L, S

183   and T; Supplemental Table S2). SCI was reduced from approximately 58% in *Gfp* plants

9

184   to 29-42% in *GfpDCL2Ai* and *GfpDCL2Bi* plants (Fig. 1U; Supplemental Table S2).

185   *DCL2* RNAi also caused a reduction in the number of silencing foci per leaf (Fig. 1R;

186   Supplemental Table S2). RNAi knock-down of *DCL1* or *DCL3* did not affect the number

187   of silencing foci and only reduced cell-to-cell movement of VIGS to a small extent, as

188   evidenced by 3-5% decreases in silencing foci sizes and/or some reductions in SCI (Fig.

189   1H-J, M, N and R-U; Supplemental Table S2). This suggests that *DCL3* and/or *DCL1*

190   may not contribute significantly to intercellular VIGS. A possible role cannot be ruled out

191   completely, however, due to discrepancy between the two *GfpDCL3i* lines, and for we

192   only have data from a single *GfpDCL1i* line. As with *DCL2* RNAi, *DCL4* RNAi caused a

193   reduction in the number of silencing foci in *GfpDCL4Ai* and *GfpDCL4Bi* plants (Fig. 1R;

194   Supplemental Table S2). This is consistent with the predominant role that *DCL4* plays in

195   intracellular VIGS. To our surprise, the average sizes of silencing foci increased by more

196   than 20% (Fig. 1O, P, S and T; Supplemental Table S2). The SCI also raised from around

197   58% in the *Gfp* controls to 70-75% in the two *GfpDCL4* RNAi lines (Fig. 1U;

198   Supplemental Table S2). These results demonstrate that *DCL4* RNAi reduced

199   intracellular silencing, but enhanced intercellular spread of VIGS. Taken together, our

200   findings show that *DCL4* RNAi enhances but *DCL2* RNAi reduces cell-to-cell spread of

201   VIGS in *Nb*.

202

DCL4 Interferes With *DCL2* to Control Intercellular VIGS

204   To investigate whether *DCL4* and *DCL2* would affect each other to influence cell-to-cell

205   spread of VIGS in *Nb*, we inoculated the triple-cross *GfpDCL24i* plant with

206   TCV/GFPΔCP. We found a marked reduction in the number of *GFP* silencing foci (Fig.

207   1R; Supplemental Table S2), consistent with the reduction in the number of silencing foci

208   observed in *GfpDCL2* RNAi and *GfpDCL4* RNAi lines. However, in the triple-cross

209   plants, the average sizes of silencing foci decreased by more than 40%, and SCI also fell

210   from 58% to 44% when compared to the *Gfp* control (Fig. 1Q, S-T; Supplemental Table

211   S2). These results demonstrate that simultaneous RNAi of both *DCL2* and *DCL4* reduced

212   both intra- and intercellular VIGS, similar to what is seen in *GfpDCL2* RNAi lines but to

213   a greater extent. The inhibition of intercellular spread of VIGS in the triple-cross

214   *GfpDCL24i* line is opposite to the increase in intercellular VIGS seen in the *GfpDCL4*
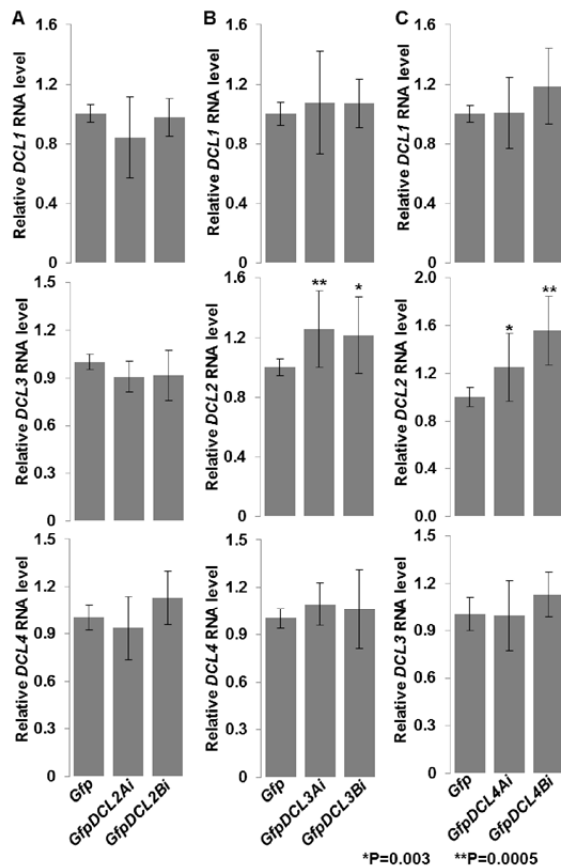
Figure 2. Regulation of *DCL2* Expression by *DCL3* and *DCL4*. (A-C) Effects of RNAi of *DCL2* (A), *DCL3* (B) and *DCL4* (C) on *DCL* gene expression. Young leaf tissues were collected at 6-8 leaf stage from four different plants of each transgenic line as indicated. RNA transcripts were analysed by qRT-PCR. Four technical replicates for qRT-PCR assays were performed on each cDNA of four biological duplicates (n = 4; leaf tissues from four different transgenic plants). Student's *t*-tests were performed for data (mean ± standard deviation) and P-values are indicated (asterisks). *DCL2i* does not affect expression of *DCL1*, *DCL3* or *DCL4* (A). However *DCL3i* (B) or *DCL4i* (C) resulted in increased mRNA levels of *DCL2*.

215   RNAi lines. This implies that *DCL4* imposed an epistatic effect on *DCL2* to affect

216   intercellular VIGS. This conclusion is supported by data from qRT-PCR assays (Fig. 2).

217   *DCL2* RNAi had no obvious impact on mRNA levels of *DCL1*, *DCL3* and *DCL4* (Fig.

218   2A). However, *DCL4* RNAi led to a 20–40% increase in *DCL2* expression but had no

11

219   substantial influence on the transcript levels of *DCL1* or *DCL3*; *DCL3* RNAi also

220   enhanced the level of *DCL2* transcripts, but did not affect expression of *DCL1* or *DCL4*

221   (Fig. 2B, C). Together with the specific RNAi effects on each *DCL* (Supplemental

222   Dataset S1), these data reveal that *DCL4* is involved in a negative regulation of *DCL2*

223   expression and as a consequence affecting the intercellular spread of VIGS in *Nb*.

224

225   ***DCLs* Play Differential Roles in vsiRNA Biogenesis**

226   To further understand how *DCLs* contribute to intra- and intercellular VIGS, we

227   performed next generation sequencing of sRNA libraries for mock- or TCV/GFPΔCP-

228   inoculated *Gfp*, *GfpDCL1i*, *GfpDCL2Ai*, *GfpDCL3Bi* and *GfpDCL4Ai* (Supplemental

229   Text S2; Supplemental Dataset S1-3; Supplemental Fig. S1). We then mapped vsiRNAs

230   and *TcvGFP* siRNAs onto the sequence of TCV/GFPΔCP (Fig. 3; Supplemental Fig. S2)

231   and TCVΔCP (Supplemental Fig. S3-4). We found abundant vsiRNAs in TCV/GFPΔCP-

232   inoculated RNAi lines (Fig. 3A-E; Supplemental Fig. S3A-E), compared to their mock

233   controls (Supplemental Fig. S2A-E; Supplemental Fig. S4A-E; Supplemental Table S3).

234   This is consistent with induction of effective VIGS in these plants (Fig. 1H-U;

235   Supplemental Table S2). More vsiRNAs were recorded in *GfpDCL1i*, *GfpDCL2Ai* and

236   *GfpDCL3Bi* plants (Fig. 3B-D; Supplemental Fig. S3B-D) than in *Gfp* controls (Fig. 3A;

237   Supplemental Fig. S3A; Supplemental Table S3). However, the reads of vsiRNAs,

238   particularly in the sense polarity, decreased in *GfpDCL4Ai* plants (Fig. 3E; Supplemental

239   Fig. S3E; Supplemental Table S3) despite a marked increase in the overall number of

240   siRNAs (vsiRNAs and *TcvGFP*-siRNAs) mapped to TCV/GFPΔCP (Supplemental Table

241   S3). These results are consistent with the reduced level of recombinant viral RNAs in

242   TCV/GFPΔCP-inoculated *DCL* RNAi plants, compared to the non-RNAi controls

243   (Supplemental Fig. S5). On the other hand, the distribution of vsiRNAs across

244   TCV/GFPΔCP (Fig. 3A-E) or TCVΔCP (Supplemental Fig. S3A-E) was identical among

245   all virus-inoculated RNAi and control plants. Taken together, these data demonstrate that

246   *DCL4* is able to efficiently target viral RNAs for the production of vsiRNAs during cell-

247   autonomous VIGS. Our results also reveal that *DCL2* is required for cell-to-cell spread of

248   VIGS, and *DCL2* could target viral RNA and *TcvGFP* mRNA for degradation in *Nb*.
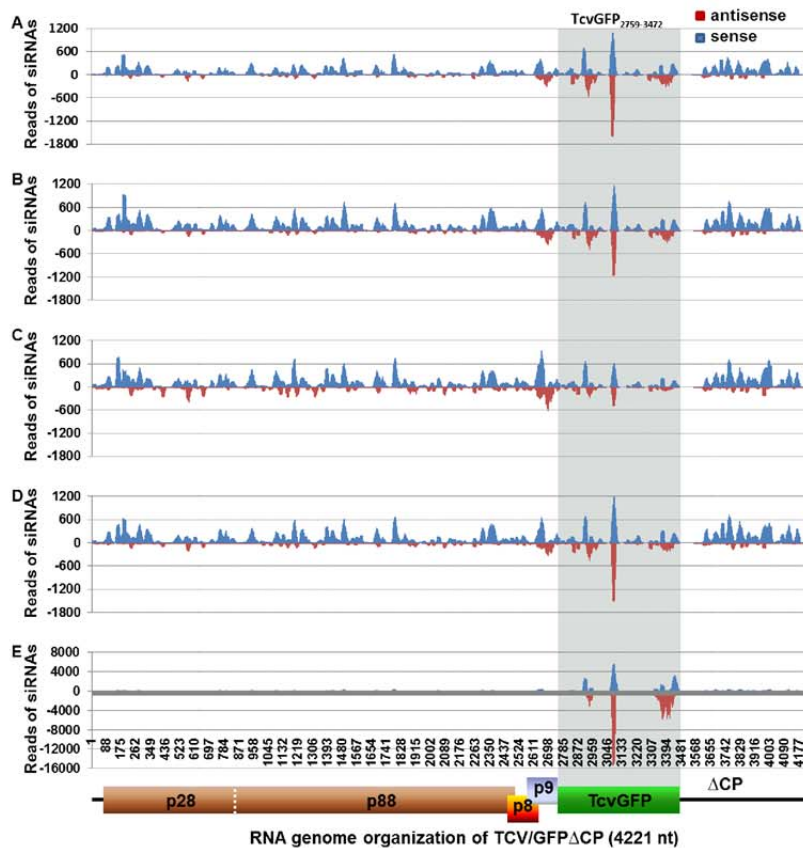
249

Figure 3. Distribution of 20-25nt vsiRNAs and siRNA$_{TcvGFP}$ across the TCV/GFPΔCP RNA. (A) *Gfp*. (B) *GfpDCL1i*. (C) *GfpDCL2Ai*. (D) *GfpDCL3Bi*. (E) *GfpDCL4Ai*. The sRNA libraries were generated from sRNA samples extracted from TCV/GFPΔCP-inoculated leaves. Blue and red bars represent siRNAs aligned to the sense (positive) and antisense (negative) strands of TCV/GFPΔCP viral RNA and *TcvGFP* mRNA (highlighted), respectively. The TCV/GFPΔCP genome organisation is indicated.

250 **Antagonistic Influences of *DCL4* and *DCL2* on Accumulation of siRNAs Associated**

251 **with Intercellular VIGS**

252 In contrast to the situation with vsiRNAs, *GfpDCL* RNAi lines differed in the generation

253 of *TcvGFP* or transgene *16cGFP* siRNAs (dubbed siRNA$_{TcvGFP}$ and siRNA$_{16cGFP}$) that are
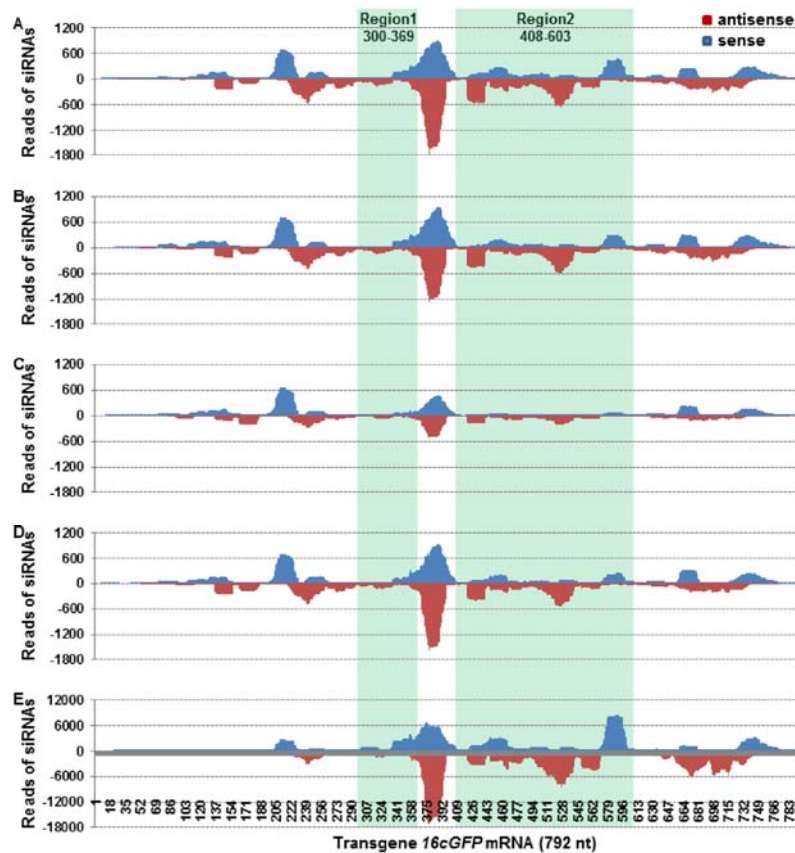
Figure 5. Distribution of 20-25nt *GFP* siRNAs across the 792nt Transgene *16cGFP* mRNA. (A) *Gfp*. (B) *GfpDCL1i*. (C) *GfpDCL2Ai*. (D) *GfpDCL3Bi*. (E) *GfpDCL4Ai*. The sRNA libraries were generated from sRNA samples extracted from TCV/GFPΔCP-inoculated leaves. Blue and red bars represent siRNAs aligned to the sense (positive) and antisense (negative) strands of *16cGFP* mRNA, respectively. The two regions (Region 1 and Region 2) having less sequence similarity with that of the transgene *TcvGFP* mRNA (see Fig. 4) as well as nucleotide coordinates are indicated.

254   associated with intra- and intercellular VIGS. Note that the 714nt *TcvGFP* (Ryabov et al.,

255   2004) and 792nt *16cGFP* (Haseloff et al., 1997; Ruiz et al., 1998) mRNAs are not

256   identical. Sequences between nucleotides 237-306 and 345-540 in *TcvGFP* (designated

257   TcvGFP$_{237-306}$ and TcvGFP$_{345-540}$) differ from the corresponding regions 300-369 and
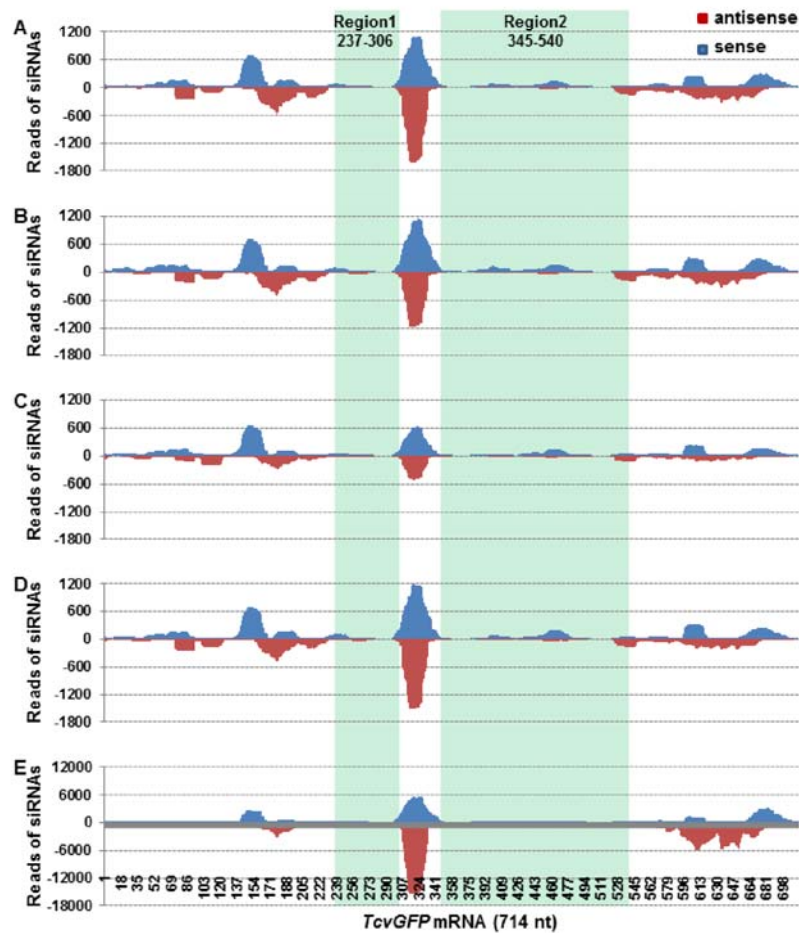
14

Figure 4. Distribution of 20-25nt *GFP* siRNAs across the 714nt *TcvGFP* mRNA. (A) *Gfp*. (B) *GfpDCL1i*. (C) *GfpDCL2Ai*. (D) *GfpDCL3Bi*. (E) *GfpDCL4Ai*. The sRNA libraries were generated from sRNA samples extracted from TCV/GFPΔCP-inoculated leaves. Blue and red bars represent siRNAs aligned to the sense (positive) and antisense (negative) strands of *TcvGFP* mRNA, respectively. The two regions (Region 1 and Region 2) having less sequence similarity with that of the transgene *16cGFP* mRNA (see Fig. 5) as well as nucleotide coordinates are indicated.

258   408-603 in *16cGFP* (designated 16cGFP$_{300-369}$ and 16cGFP$_{408-603}$) (Supplemental Fig. S6).

259   Compared to the *Gfp* control and *GfpDCL1i* and *GfpDCL3Bi* plants, the levels of

260   siRNA$_{TcvGFP}$ and siRNA$_{16cGFP}$ were reduced in *GfpDCL2Ai*, but significantly increased in

261   *GfpDCL4Ai* (Supplemental Table S3). We then mapped the siRNAs onto *TcvGFP* (Fig. 4;

15

262 Supplemental Fig. S7) and *16cGFP* mRNA (Fig. 5; Supplemental Fig. S8). The

263 distribution of sense and antisense *GFP* siRNAs to regions that are identical in *TcvGFP*

264 and *16cGFP* was essentially the same in *Gfp* and in each of the *DCL* RNAi lines,

265 however, the levels of siRNA$_{TcvGFP}$ and siRNA$_{16cGFP}$ were lower in *GfpDCL2Ai*, and

266 much higher in *GfpDCL4Ai*, compared to *Gfp*, *GfpDCL1i* and *GfpDCL3Bi* (Fig. 4A-E;

267 Fig. 5A-E; Supplemental Table S3). Moreover in *GfpDCL4Ai* the level of siRNA$_{16cGFP}$

268 (2.5 million reads) was approximately double compared to the abundance of siRNA$_{TcvGFP}$

269 (1.28 million reads) (Supplemental Table S3). Such substantial differences between

270 siRNA$_{TcvGFP}$ and siRNA$_{16cGFP}$ levels suggest that the transgene *16cGFP* mRNA was

271 targeted and diced by intra- and intercellular VIGS to a greater extent than *TcvGFP*

272 transcripts. In contrast, different profiles were observed for siRNA$_{TcvVGFP}$ and

273 siRNA$_{16cGFP}$ corresponding to the two less-similar regions (Region 1: TcvGFP$_{237-306}$ and

274 16cGFP$_{300-369}$; Region 2: TcvGFP$_{345-540}$ and 16cGFP$_{408-603}$) (Fig. 4A-E; Fig. 5A-E).

275 TcvGFP$_{237-306}$ and TcvGFP$_{345-540}$ siRNAs were of low abundance and generally of sense

276 polarity in the control and all RNAi lines (Fig. 4A-E). However, higher levels of

277 16cGFP$_{300-369}$ and 16cGFP$_{408-603}$ siRNAs were observed, a significant amount of which

278 was antisense. As with the other GFP siRNAs, the levels of 16cGFP$_{300-369}$ and 16cGFP$_{408-}$

279 $_{603}$ siRNAs were much higher in *GfpDCL4Ai* and lower in *GfpDCL2Ai*, compared to *Gfp*,

280 *GfpDCL1i* and *GfpDCL3Bi* (Fig. 5A-E).

281 These results demonstrate that *DCL4* and *DCL2* antagonistically affected the

282 accumulation of siRNAs associated with intercellular VIGS. The reduction of

283 siRNA$_{TcvGFP}$ and siRNA$_{16cGFP}$ in *GfpDCL2Ai* or the massive accumulation of these

284 siRNAs in *GfpDCL4Ai* is likely to be due to the respective loss or gain-of-function of

285 DCL2-dependent production of primary or secondary siRNAs in these RNAi lines.

286

Potential DCL2-processed/dependent siRNA Signals for Intercellular VIGS

288 In *Nb*, the DCL2-processed siRNAs (Fig. 4C; Fig. 5C) and/or DCL2-dependent siRNAs

289 (produced by *DCL2*-activated pathways; Fig. 4E; Fig. 5E) are likely to be involved in the

290 intercellular spread of epidermal cell-originating VIGS. Consistent with this idea, an

291 elevated level of 22nt siRNAs was only found in TCV/GFPΔCP-inoculated *GfpDCL4Ai*

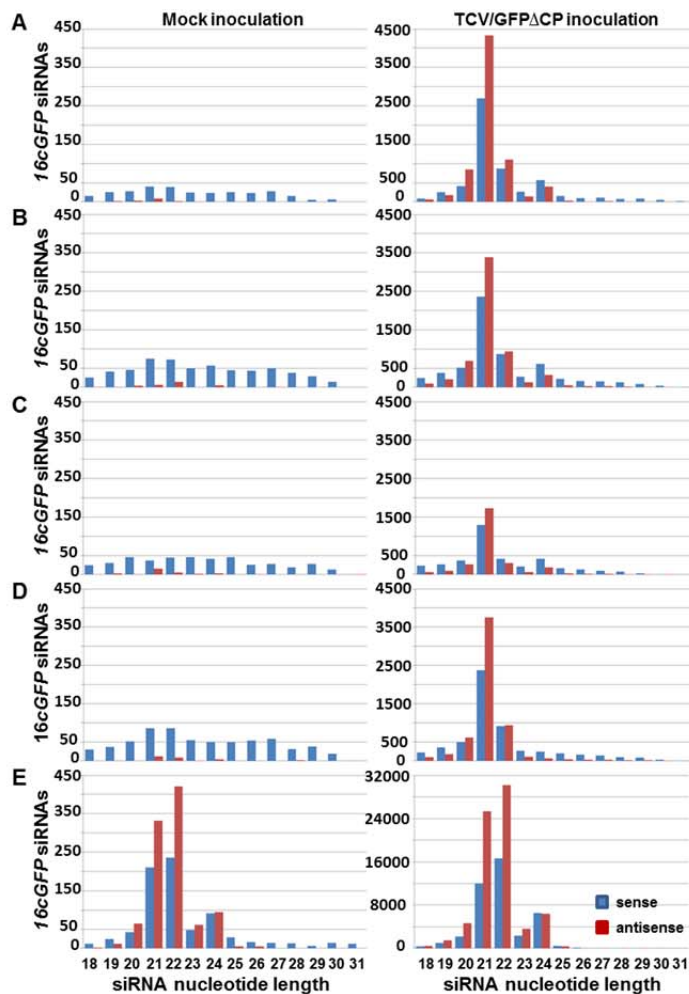292 and *GfpDCL4Bi* plants that exhibited increased intercellular VIGS (Fig. 1; Supplemental

Figure 6. Size Profiles of Transgene *GFP* siRNA$_{16cGFP}$. (A) *Gfp*. (B) *GfpDCL1i*. (C) *GfpDCL2Ai*. (D) *GfpDCL3Bi*. (E) *GfpDCL4Ai*. The sRNA libraries were generated from sRNA samples extracted from leaves with mock (left) or TCV/GFPΔCP (right) inoculation. Blue and red bars represent siRNAs aligned to the sense and antisense strands of the transgene *16cGFP* mRNA respectively.

293   Fig. S9). To examine this correlation further, we analyzed the size profiles of sense and

294   antisense siRNA$_{16cGFP}$ (Fig. 6). The 21, 22 and 24nt siRNA$_{16cGFP}$ displayed similar size-

295   profiles between *Gfp* and *GfpDCL1i* (Fig. 6A and B, right panel). There was an obvious

296   reduction in 24nt siRNA$_{16cGFP}$ in *GfpDCL3Bi* (Fig. 6D, right panel). However among *Gfp*,

297   *GfpDCL1i* and *GfpDCL3Bi*, the 21nt siRNA$_{16cGFP}$ was always dominant while the levels

298   of 22nt siRNAs remained similar (Fig. 6A, B and D, right panel; Supplemental Table S4).

299   These findings further indicate that *DCL1*, *DCL3*, and DCL3-processed 24nt siRNAs

300   may not significantly contribute to cell-to-cell spread of VIGS, consistent with the results

301   of the local silencing assays (Fig. 1H-U).

302   RNAi of *DCL2* or *DCL4* imposed contrasting effects on the accumulation of 21,

303   22 and 24nt siRNA$_{16cGFP}$. Compared to *Gfp*, *GfpDCL1i* and *GfpDCL3Bi* (Fig. 6A, B and

304   D, right panel), the absolute reads of 21, 22 and 24nt siRNA$_{16cGFP}$ reduced in *GfpDCL2Ai*

305   (Fig. 6C, right panel), and markedly increased in *GfpDCL4Ai* (Fig. 6E, right panel).

306   Nonetheless, the percentage of the 22nt siRNA$_{16cGFP}$ decreased in *GfpDCL2Ai* whilst the

307   relative abundance of 21nt siRNA$_{16cGFP}$ reduced in *GfpDCL4Ai* (Supplemental Table S4).

308   These are in accordance with the respective roles of DCL4 and DCL2 in 21 and 22nt

309   siRNA biosynthesis. The levels of DCL2-processed 22nt siRNA$_{16cGFP}$ and DCL2-

310   dependent siRNA$_{16cGFP}$ were particularly low in *GfpDCL2Ai* (Fig. 6C, right panel), but

311   copious in *GfpDCL4Ai* (Fig. 5E, right panel; Supplemental Table S4), consistent with the

312   observed attenuation or enhancement of intercellular VIGS in the RNAi plants

313   respectively (Fig. 1). We also analyzed the size profiles of sense and antisense vsiRNA

314   (Fig. 7). Distributions of 18–31-nt vsiRNAs were not obviously altered among *Gfp*,

315   *GfpDCL1i*, *GfpDCL2Ai* and *GfpDCL3Bi* (Fig. 7A-D, right panel). In these RNAi lines,

316   the majority of vsiRNAs were 21nt in length (Fig. 7; Supplemental Table S4). However

317   in *GfpDCL4Ai*, vsiRNAs shifted their sizes largely to 22nt although there were also

318   marked increases in 21 and 24nt vsiRNAs (Fig. 7E, right panel). Notably, there was an

319   approximate 10% reduction of 22-nt vsiRNAs in *GfpDCL2Ai* compared to the *Gfp*

320   control (Supplemental Table S4). Taken together, our data show that *DCL4* plays a major,

321   and *DCL2* a minor, role in producing 21 or 22nt vsiRNAs for intracellular VIGS, whilst

322   *DCL2* is required to generate and perceive DCL2-processed/dependent mobile signals for

323   intercellular VIGS. These conclusions are further supported by similar results that were

324   generated from six extra sRNA libraries for the *Gfp* control and two different RNAi lines

325   *GfpDCL2Bi* and *GfpDCL4Bi* (Supplemental Fig. S10A-E).
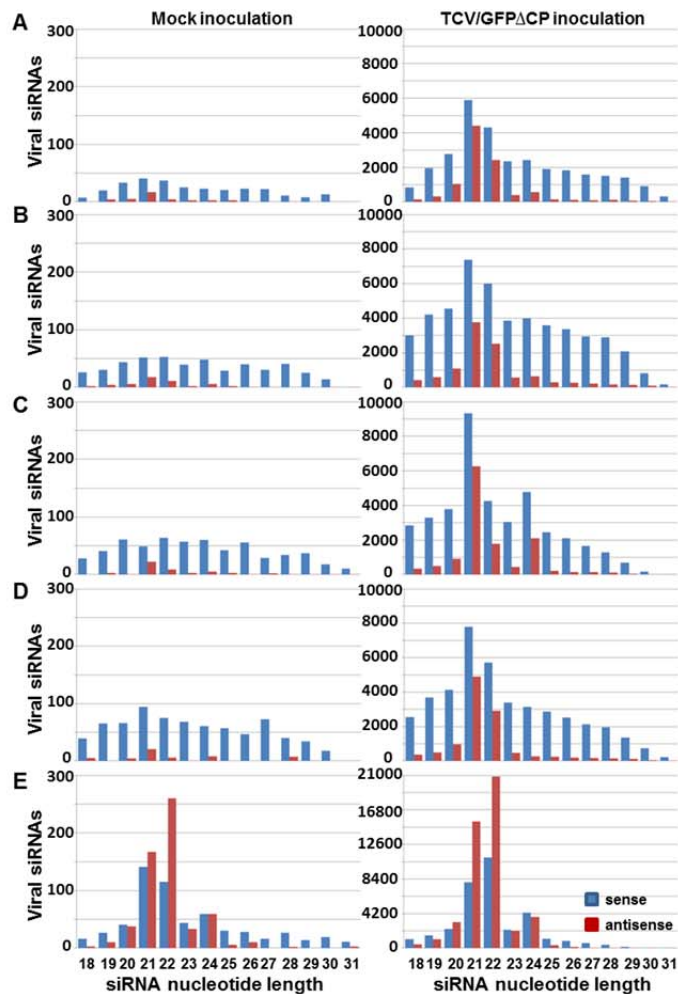
326

327

Figure 7. Size Profiles of TCV/GFPΔCP Viral siRNAs. (A) *Gfp*. (B) *GfpDCL1i*. (C) *GfpDCL2Ai*. (D) *GfpDCL3Bi*. (E) *GfpDCL4Ai*. The sRNA libraries were generated from sRNA samples extracted from leaves with mock (left) or TCV/GFPΔCP (right) inoculation. Blue and red bars represent siRNAs aligned to the sense and antisense strands of TCV/GFPΔCP RNA, respectively.

DISCUSSION

329 In plants, *DCLs* play diverse roles in sense- and hairpin RNA-mediated PTGS and TGS

330 (Parent et al., 2015; Mlotshwa et al., 2008; Xie et al., 2004; 2005). *DCL4*, *DCL2* and their

331 cognate 21 and 22nt vsiRNAs are involved in cell-autonomous VIGS but their antiviral

19

332   functioning roles are debated (Bouche et al., 2006; Fusaro et al, 2006; Garcia-Ruiz et al,

333   2010; Qu et al., 2008).

334   In this study, we reveal several interesting findings:

335   (1) RNAi of the four *DCL* genes does not affect cell-to-cell movement deficiency

336   of the immobile virus TCV/GFPΔCP (Fig.1). This is consistent with our previous report

337   that compromising of silencing machinery alone was not sufficient to promote virus

338   movement (Shi et al., 2009). These findings ensure that any intercellular VIGS that we

339   observe in our assays do not result from cell-to-cell movement of the recombinant viral

340   RNA, and also argue against the idea that an altered ability to establish intra- and

341   intercellular VIGS in these *DCL* DNAi lines may enable TCV-GFPΔCP to move locally

342   or systemically more than in wild-type *Nb* plants.

343   (2) *DCL4* inhibited non-cell autonomous intercellular VIGS whilst it acted as a

344   major trigger for intracellular VIGS (Fig. 3), consistent with its critical role in cell-

345   autonomous silencing and vsiRNA biogenesis (Wang et al., 2011; Xie et al., 2005). Our

346   findings are also in agreement with previous reports that *dcl4* mutations enhance

347   transitivity of cell-autonomous PTGS and can rescue phloem-originating PTGS in

348   *Arabidopsis* (Mlotshwa et al., 2008; Parent et al., 2015). The fact that *DCL4* attenuates

349   intercellular VIGS implies that DCL4-processed 21nt vsiRNAs are unlikely to be

350   involved in cell-to-cell spread of VIGS in *Nb*.

351   (3) *DCL2*, probably along with DCL2-processed/dependent siRNAs and their

352   precursor RNAs, is involved in intercellular VIGS. *DCL2* was also able to target and

353   degrade viral RNAs in plant cells but this activity was largely redundant when functional

354   *DCL4* was present (Fig. 3). These findings suggest that *DCL2* could influence

355   intracellular VIGS in *Nb* although *DCL2* is thought to be dispensable for antiviral

356   silencing in *Arabidopsis* (Wang et al., 2011). Neither *DCL1* nor *DCL3* affected vsiRNA

357   production or intra- and intercellular VIGS. Intriguingly, *DCL2* played a key role in

358   spreading VIGS from individual epidermal cell to adjacent epidermal and mesophyll cells,

359   a formerly unidentified function in silencing-based antiviral defense.

360   (4) Silencing machinery degraded *TcvGFP* mRNA and the resultant siRNA$_{TcvGFP}$

361   targeted identical regions in the transgene *16cGFP* mRNA and generated siRNA$_{16cGFP}$ for

362   intracellular VIGS in TCV/GFPΔCP-infected epidermal cells (Figs. 4-7). Such

363   siRNA$_{TcvGFP}$ and siRNA$_{16cGFP}$ in sense and antisense polarities then led to biogenesis of

364   siRNAs associated with different parts across the *16cGFP* and *TcvGFP* RNA sequences

365   for intra- and intercellular VIGS. Our results thus imply that initial signals for

366   intercellular VIGS might consist of sense and antisense siRNA$_{TcvGFP}$ and siRNA$_{16cGFP}$.

367   Production of such signals in incipient epidermal cell (*i.e.* the TCV/GFPΔCP-infected

368   cell) and subsequent induction of *16cGFP* silencing in neighboring recipient cells (*i.e.*

369   TCV/GFPΔCP non-infected cells) were influenced positively by *DCL2*, but negatively by

370   *DCL4* (Fig. 1; Fig. 2). However, in contrast to complete loss-of-function genetic mutants,

371   RNAi lines are partial loss of function. It is also possible that TCV/GFPΔCP infection

372   could alter the expression of the *DCL* genes targeted by RNAi. Sequenced small RNAs

373   were from all of the cells in the inoculated leaves, including the inducing and recipient

374   cells. Considering these factors, it remains possible that long dsRNA precursors of DCL2

375   (or DCL4) could move between cells or long distance for induction of non-cell

376   autonomous VIGS.

377   Collectively, our results suggest that *DCL4* and *DCL2* play major but distinct

378   roles in intra-/intercellular VIGS. Involvement of *DCL2* and DCL2-processed/dependent

379   siRNAs as well as their precursor RNAs in intercellular VIGS is consistent with the fact

380   that DCL2 and DCL2-processed 22nt siRNA can effectively trigger biogenesis of

381   secondary siRNAs in plants (Chen et al., 2010), and restore intercellular PTGS induced

382   by sense- and hairpin-transgene RNAs in the *Arabidopsis dcl4* mutant (Mlotshwa et al.,

383   2008; Parent et al., 2015). It should be pointed out that silencing spread in our system is

384   more complex than other systems since it is dependent on the expression of both p8 and

385   p9 proteins of TCV (Zhou et al., 2008). Therefore, we are cautious to expand our findings

386   to other examples of cell-to-cell spread of RNA silencing, such as the controversial

387   *Arabidopsis* model in which, *DCL4* and DCL4-processed 21-nt siRNAs are thought to be

388   directly involved in short-range cell-to-cell spread of phloem-originating PTGS.

389   Nevertheless, our findings support a hypothesis that *DCL4* is essential for cell-

390   autonomous intracellular VIGS, but negatively regulates intercellular VIGS. This is likely

391   to be achieved via *DCL4*-mediated epistatic interference over *DCL2* because the latter is

392   essential to promote cell-to-cell spread of VIGS. Indeed *DCL4* can suppress the

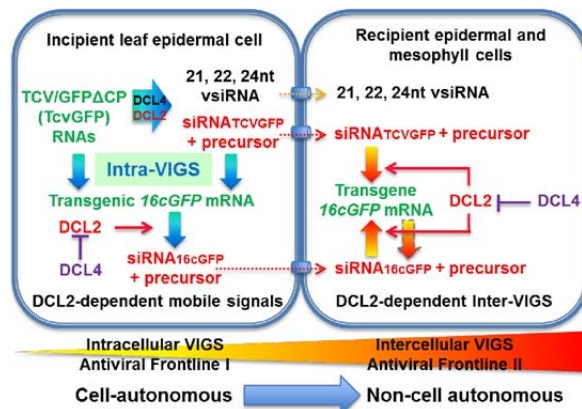393   expression of *DCL2* in *Nb* (Fig. 2). *DCL2* is also required to generate and perceive

Figure 8. Cell- and Non-cell Autonomous VIGS in *N. benthamiana*. In incipient leaf epidermal cells (*i.e.* individual cells initially infected by TCV/GFPΔCP), *DCL4* plays a critical role in biogenesis of vsiRNAs, siRNA$_{TCVGFP}$ and transgene siRNA$_{16cGFP}$. These siRNAs are associated with cell-autonomous intracellular VIGS (Intra-VIGS) to inhibit local virus infection. DCL4-processed siRNAs are unlikely involved in spread of VIGS from leaf epidermal cell to adjacent cells because *DCL4* inhibits intercellular VIGS. In the incipient cell, *DCL2* can also target and dice viral RNAs, *TcvGFP* and *16cGFP* mRNA into siRNAs, but this activity is largely blocked by *DCL4* (**T** sign). In contrast, the key functionality of *DCL2* is to trigger efficient intercellular VIGS (Inter-VIGS). This is likely achieved through its activities to produce DCL2-processed/dependent siRNAs (and/or their precursor long RNAs, highlighted red) in incipient cells and to perceive these mobile signals for non-cell autonomous inter-VIGS in recipient epidermal and mesophyll cells. Neither *DCL1* nor *DCL3* affects vsiRNA production, intra- and intercellular VIGS. Thus *DCL4* and *DCL2* play major but distinct roles in cell- and non-cell autonomous VIGS that form a dual antiviral frontline in incipient and recipient cells. *DCL4*, the primary defender for the cell-autonomous intracellular VIGS, can attack viruses within the initially infected cells. However, if viruses break through this defence frontline, non-cell autonomous intracellular VIGS can efficiently spread to nearby recipient cells. This is due to loss of the negative control of intercellular VIGS mediated by *DCL4*. Intercellular VIGS is dependent upon functional *DCL2* and DCL2-processed/dependent siRNAs (and/or their precursor long RNAs), but it is negatively controlled by *DCL4*. RNAi of *DCL4* results in fully functional *DCL2* that enhances cell-to-cell spread of VIGS. The intercellular VIGS can then defend recipient cells from further virus infection. Such a dual-defence strategy can compensate each other to give host cells evolutionary advantage to battle against virus infection. This model is relevant to virus-VIGS interaction at the intra-/intercellular level, rather than to systemic virus infection. The potential spread of DCL2-processed/dependent siRNAs (and their precursor long RNAs, highlighted red) to move from the incipient to recipient cell through plasmodesmata is indicated with dashed arrows and cylinder signs.

mobile signals for systemic PTGS whilst *DCL4* inhibits systemic PTGS (Fan et al., 2017, under revision). To put these findings in the context of RNA silencing-based defence, we propose two separate components of an integrated viral defence strategy in which *DCL2* and *DCL4* play different roles (Fig. 8). *DCL4*, the primary defender in the cell-

398 autonomous intracellular VIGS, attacks viruses within the initially infected cells.

399 Simultaneously it also inhibits non-cell autonomous silencing. Thus, if this intracellular

400 VIGS frontline in incipient cells was broken, for example through inhibiting *DCL4*

401 activity by VSR such as P1/HC-Pro and P38 (Csorba et al., 2015; Mlotshwa et al, 2008),

402 intercellular VIGS would then be activated efficiently spreading to nearby recipient cells

403 to form a second frontline against the virus. Non-cell autonomous intercellular VIGS

404 relies upon functional *DCL2* and DCL2-processed/dependent siRNAs and their precursor

405 RNAs. In this scenario, *DCL2* is required to trigger the intercellular VIGS frontline and

406 defend recipient cells from further virus invasion. *DCL2* may also contribute to cell-

407 autonomous VIGS, but *DCL2* can only fulfil this activity when *DCL4* is absent or

408 dysfunctional. This explains why an increased intercellular VIGS was observed in *DCL4*

409 RNAi plants, but a deceased non-cell autonomous VIGS in *DCL2* RNAi plants. Such a

410 local dual-defence strategy would be more difficult for the virus to breakdown and may

411 provide plants with an evolutionary advantage in their defence against viral pathogens

412 (Supplemental Text S3).

413

414 **MATERIALS AND METHODS**

415 **Plant Materials and Growth Conditions**

416 Wild-type *Nicotiana benthamiana* (*Nb*) and transgenic lines (Supplemental Table S1)

417 were grown and maintained in insect-free growth-rooms at 25°C with supplementary

418 lighting to give a 16-hour photoperiod.

419

420 **Plasmid Constructs, Virus Inoculation and Microscopy**

421 Construction of TCV/GFPΔCP was previously described (Ryabov et al., 2004). The full-

422 length GFP sequence was PCR amplified using TCV/GFPΔCP as DNA template and

423 cloned into pMD18-T (Takara) to produce pT7.GFP construct from which *GFP* RNA

424 transcripts were produced by *in vitro* transcription using T7 RNA polymerase. Primers

425 used for making this construct are listed in Supplemental Table S5. TCV/GFPΔCP RNA

426 was generated by *in vitro* transcription and used to mechanically inoculate *Nb*, *DCL*

427 RNAi, *16cGFP*, *Gfp*, *GfpDCL* RNAi plants as described (Ryabov et al., 2004).

428   Inoculated leaves were collected and visualized under a Zeiss Axiphot microscope as

429   described (Ryabov et al., 2004).

430

431   **Intra- and Intercellular VIGS Assays**

432   We used a cell-specific, silencing suppression-free and movement-deficient Turnip

433   crinkle virus (TCV/GFPΔCP)-based system to induce intracellular VIGS in a single

434   epidermal cell, from which silencing spreads to form visible silencing foci covering 100-

435   300 epidermal cells, equivalent to a circular area with a radius of 6-10 epidermal cells, on

436   the leaf epidermis of transgenic *16cGFP* plants (Qin et al., 2012; Ryabov et al., 2004;

437   Zhou et al., 2008). Of important notes, the precise location of a single epidermal cell that

438   was initially infected with the movement-defective TCV/GFPΔCP could not be located

439   prior to development of a visible silencing focus from the infected cell. Due to the

440   compact TCV genome organization and viral gene expression strategy (Carrington et al.,

441   1989; Cohen et al., 2000), it would be almost impossible to clone a second reporter gene,

442   in addition to *GFP*, into TCV/GFPΔCP as an extra marker for measuring the initial

443   infection of individual epidermal cell. Nevertheless, visible *GFP* silencing foci are a good

444   indicator for induction and spread of TCV/GFPΔCP-induced intracellular VIGS. Upon

445   mechanic inoculation, their appearance is a gradual process starting from the individual

446   cell on the upper epidermises which is initially infected by TCV/GFPΔCP. Intracellular

447   *GFP* silencing is induced by TCV/GFPΔCP in the single epidermal cell; and

448   subsequently moves horizontally and vertically to neighboring upper epidermal,

449   mesophyll and lower epidermal cells in a three-dimensional manner, i.e. occurrence of

450   intercellular VIGS (Qin et al., 2012; Zhou et al., 2008).

451   To perform intra- and intercellular VIGS assays, a single young leaf (2nd from top)

452   of each of four-to-six seedlings (six-leaf stage) of *16cGFP*, *Gfp GfpDCL1i*, *GfpDCL2Ai*,

453   *GfpDCL2Bi*, *GfpDCL3Ai*, *GfpDCL3Bi*, *GfpDCL4Ai* or *GfpDCL4Bi* lines were

454   mechanically inoculated with an equal amount of RNA transcripts produced by *in vitro*

455   transcription from 2.5-µg *Pac*I-linearized TCV/GFPΔCP plasmid DNA as described

456   (Ryabov et al., 2004). Induction and spread of *GFP* silencing was routinely examined

457   under long-wavelength UV light and recorded photographically using a Nikon Digital

458   Camera D7000. Regions of leaf lamina in which silencing of *GFP* mRNA occurred show

459 red chlorophyll fluorescence, while tissues expressing GFP show green fluorescence

460 under long-wavelength UV light. Numbers and sizes of *GFP* silencing foci (dark patches)

461 were counted, measured and photographed under a Zeiss Axiphot microscope using

462 settings to visualize GFP green fluorescence as described (Qin et al., 2012). Number of

463 silencing foci on an individual leaf was normalized against the average number of

464 silencing foci per leaf of the control plants (i.e. *16cGFP* as control for *GfpDCL1i*, and

465 *Gfp* as control for *GfpDCL2Ai*, *GfpDCL2Bi*, *GfpDCL3Ai*, *GfpbDCL3Bi*, *GfpDCL4Ai*,

466 *GfpDCL4Bi* and *GfpDCL24i*) to minimize disparities that could be caused by

467 experimental variations such as leaf sizes among different plants and freshly-generated

468 inoculum RNA transcripts used in different experiments. SCI was calculated as

469 percentage between the numbers of silencing foci counted on lower and upper (inoculated

470 side) epidermises. Intra- and intercellular VIGS assays were performed for each of the

471 transgenic lines in at least two separate experiments.

472

473 **RNA Extraction and Northern Hybridization**

474 For quantitative Real-Time PCR (qRT-PCR), total RNAs were extracted from leaf tissues

475 using the RNAprep Pure Plant Kit (Tiangen) as recommended by the manufacturer. For

476 Northern blot, total RNAs were extracted from leaf tissues with Trizol reagent

477 (Invitrogen, Carlsbad, CA) as recommended by the manufacturer. To analyze siRNAs,

478 low-molecular-mass small RNAs were enriched from total RNA as previously described

479 (Hamilton and Baulcombe, 1999). The enriched small RNAs (2.5µg) were fractionated

480 on an 18% denaturing polyacrylamide–7 M urea gel in 1 x Tris–borate–EDTA (TBE)

481 buffer. Small RNAs were transferred to Hybond-N+ membranes (Amersham

482 Biosciences) by upward capillary transfer in 20xSSC buffer, then cross-linked to the

483 membranes with an UVP CX 2000 UV Crosslinker for 4 times (upside, underside, upside,

484 underside) at 120 millijoules/cm^2, 1 minute each time. The membranes were hybridized

485 with digoxigenin (Dig)-labelled *GFP* RNA probes prepared by in vitro transcription

486 using pT7.GFP and DIG RNA Labeling Kit (Roche) as recommended by the

487 manufacturer. The hybridization chemiluminescence signals were detected with a

488 ChemiDoc^{TM} XRS+ imaging System (Bio Rad).

489

qRT-PCR

491 TCV/GFPΔCP or mock-inoculated leaves of *Nb*, *DCL* RNAi, *16cGFP, Gfp*, and *GfpDCL*

492 RNAi plants were taken at 7 days post inoculation in three repeated experiments for RNA

493 extraction. The first-stranded cDNA was synthesized using total RNAs treated with

494 RNase-free DNase I as templates by the M-MLV Reverse Transcriptase (Promega). The

495 qRT–PCR analyses of *DCLs* mRNA or TCV/GFPΔCP RNA levels were performed using

496 specific primers (Supplemental Table S5) and the SYBR Green Mix, The amplification

497 program for SYBR Green I was performed at 95ºC for 10 seconds, 58ºC for 30 seconds

498 and 72ºC for 20 seconds on the CFX96 machine (Bio-Rad), following the manufacturer's

499 instructions. Quadruplicate quantitative assays (four technical replicates) were performed

500 on cDNA of each of three-four biological duplicates (leaf tissues from three-four different

501 treated plants). The relative RNA quantification was calculated using the formula $2^{-\Delta\Delta Ct}$

502 and normalized to the amount of GAPDH (Genbank accession number TC17509) as

503 described (Qin et al., 2012).

504

505 **Construction of sRNA Library and sRNA Sequencing**

506 Fragments of 18-30 bases long RNA were isolated from total RNA extracted from mock-

507 or TCV/GFPΔCP-inoculated leaf tissues of 3-4 different plants collected at seven days

508 post-inoculation (dpi) after being separated through 15% denaturing PAGE. Then sRNAs

509 were excised from the gel and sequentially ligated to 3'- and 5'-adapters. After each

510 ligation step, sRNAs were purified after 15% denaturing PAGE. The final purified

511 ligation products were reversely transcribed into cDNA using reverse transcriptase

512 (Finnzymes Oy). The first strand cDNA was PCR amplified using Phusion* DNA

513 Polymerase (Finnzymes Oy). The purified DNA fragments were used for clustering and

514 sequencing by Illumina Hiseq 2000 (Illumina, San Diego, CA) at the Beijing Genomics

515 Institute, Shenzhen. It should be noted that a pool of leaves from 3-4 different plants was

516 used for construction of each sRNA library. This avoided potential variations between

517 individual treated plants, in particular these for TCV/GFPΔCP-based intra- and

518 intercellular VIGS assays due to some variations of TCV/GFPΔCP replication in different

519 plants.

520

Bioinformatics Analysis of sRNA Sequences

Illumina HighSeq 2000 sequencing produced 11 to 12 million reads per sRNA library.
The reads were cropped to remove adapter sequences and were aligned to the reference
sequences using Bowtie2 (Langmead and Salzberg, 2012; Ryabov et al., 2014). The
reference sequences included TCV/GFPΔCP, viral *TcvGFP* and *16cGFP* transgene
(Haseloff et al., 1997; Ruiz et al., 1998; Ryabov et al., 2004), *DCL1*, *DCL2*, *DCL3* and
DCL4 gene sequences (Nakasugi et al., 2013) and the set of 50 tobacco microRNAs
identified in *Nicotiana* plants (Nakasugi et al., 2014; Pandey et al., 2008). SAMtools
pileup was used to produce the siRNA and miRNA coverage profiles. For correlation
analyses for the six small RNA libraries, we determined numbers of the miRNA hits
corresponding to the previously identified set of 50 *Nicotiana* miRNAs (Nakasugi et al.,
2014; Pandey et al., 2008). All analyzed small RNA libraries contained similar
proportions of host-encoded miRNA reads (Supplemental Dataset S1; Supplemental
Dataset S2; Supplemental Dataset S3), indicating equivalence and direct comparability of
the sRNA datasets. Indeed outcomes of comparisons between normalized siRNAs
generated from target sequences against the total sRNA reads for all the libraries (per 10
million sRNA reads) are consistent with that the reads of siRNAs were directly
compared.

Statistical Analysis

Normalized number of RNA silencing foci per leaf, sizes of RNA silencing foci,
"silencing cell-to-cell-spread index" (SCI) and qRT-PCR data between control and
various treatments were analysed by Student's *t*-Tests using an online programme
(http://www.physics.csbsju.edu/stats/t-test.html). It is worthwhile noting that
approximately 4% or more change in the silencing foci sizes is of statistical significance
due to the large numbers of samples (80-560) tested between wild-type controls and
RNAi lines (Fig. 1; Supplemental Table S2).

Supplemental Data

The following materials are available in the online version of this article.

Supplemental Text S1. Parameters for Assessing Intra- and Intercellular VIGS.

552   **Supplemental Text S2.** *DCLs* Play Differential Roles in vsiRNA Biogenesis**.**

553   **Supplemental Text S3.** Local VIGS vs Virus Interaction at the Intra-/intercellular Level.

554   **Supplemental Figure S1.** Total small RNA Profiles.

555   **Supplemental Figure S2.** Distribution of vsiRNAs and siRNA$_{TcvGFP}$ across the

556   TCV/GFPΔCP RNA.

557   **Supplemental Figure S3.** Distribution of vsiRNAs across the TCVΔCP RNA.

558   **Supplemental Figure S4.** Distribution of vsiRNAs across the TCVΔCP RNA.

559   **Supplemental Figure S5.** Impact of *NbDCLi* on TCV/GFPΔCP RNA Replication.

560   **Supplemental Figure S6.** Comparisons between Transgene *16cGFP* and Viral *TcvGFP*

561   Sequences.

562   **Supplemental Figure S7.** Distribution of 20-25nt *GFP* siRNAs Across the 714nt

563   *TcvGFP* mRNA.

564   **Supplemental Figure S8.** Distribution of 20-25nt *GFP* siRNAs Across the 792nt

565   Transgene *16cGFP* mRNA.

566   **Supplemental Figure S9.** Northern Detection of TCV/GFPΔCP siRNAs.

567   **Supplemental Figure S10.** *NbDCL2* and NbDCL2-dependent siRNAs for Non-cell

568   Autonomous Intercellular VIGS.

569   **Supplemental Table S1.** *NbDCL* RNAi Lines Used in This Study.

570   **Supplemental Table S2.** Impact of *DCL* RNAi on Cell-to-cell Spread of Virus-induced

571   RNA Silencing.

572   **Supplemental Table S3.** Percentage of *16cGFP* and TCV/GFPΔCP 21-, 22- and 24-nt

573   siRNA.

574   **Supplemental Table S4.** Summary of Total Viral and/or GFP siRNAs in Mock- or

575   TCV/GFPΔCP-inoculated Leaves.

576   **Supplemental Table S5.** Primers Used in This Study.

577   **Supplemental Dataset S1.** Summary of sRNA and miRNA reads.

578   **Supplemental Dataset S2**. Correlation analyses of miRNA profiles among 10 sRNA

579   libraries.

580   **Supplemental Dataset S3.** Comparisons of miRNAs among ten sRNA libraries.

581

582   **ACKNOWLEDGEMENTS**

583 We are grateful to David Baulcombe for his kind gift of the transgenic line *16cGFP* and

584 *RDR6i* seeds. The corresponding author thanks Dr Alison Tör for checking English

585 grammar and style throughout the manuscript.

586

587 **FIGURE LEGENDS**

588 **Figure 1. Different Roles of *DCLs* in the Cell-to-cell Spread of VIGS.** (A) Down-

589 regulation of *DCL* expression by RNAi. Young leaves were collected from *DCL* RNAi

590 plants at 7 days post-inoculation (dpi), and the level of *DCL* RNAs was analysed by qRT-

591 PCR. (B) Schematic of the intracellular RNA silencing trigger TCV/GFPΔCP. The T7

592 promoter, viral RNA-dependent RNA polymerases (P28, P88), movement proteins (P8

593 and P9) and GFP are indicated. (C-G) Restricted localization of TCV/GFPΔCP in single

594 epidermal cell of *Nb* (C), *DCL1i* (D) *DCL2Ai* (E), *DCL3Bi* (F) and *DCL4Ai* (G) plants.

595 (H-Q) Intercellular *GFP* silencing foci (dark patches indicated by red arrows).

596 Photographs of silencing foci on leaves of *16cGFP* (H); *GfpDCL1i* (I); *Gfp* (J);

597 *GfpDCL2Ai* (K) and *GfpDCL2Bi* (L); *GFPDCL3Ai* (M) and *GfpDCL3Bi* (N);

598 *GfpDCL4Ai* (O) and *GfpDCL4Bi* (P); and a triple-cross line *GfpDCL24i* (Q), were taken

599 under a fluorescent microscope at 7 dpi. Bar=500μm. (R) Normalized number of *GFP*

600 silencing foci per upper epidermis. Silencing foci were counted at 7 dpi from 3-21

601 different plant leaves inoculated with TCV/GFPΔCP. (S) and (T) Average size

602 (diameters, S) and percentage change (T) of silencing foci. 80-560 silencing foci on

603 different upper epidermises were randomly selected and measured. (U) SCI calculated as

604 percentage of number of silencing foci on lower epidermis out of the number of silencing

605 foci on upper epidermis. Student's *t*-tests were performed for qRT-PCR and silencing

606 data (mean ± standard deviation) and P-values are indicated (asterisks).

607

608 **Figure 2. Regulation of *DCL2* Expression by *DCL3* and *DCL4*.** (A-C) Effects of RNAi

609 of *DCL2* (A), *DCL3* (B) and *DCL4* (C) on *DCL* gene expression. Young leaf tissues were

610 collected at 6-8 leaf stage from four different plants of each transgenic line as indicated.

611 RNA transcripts were analysed by qRT-PCR. Four technical replicates for qRT-PCR

612 assays were performed on each cDNA of four biological duplicates (n = 4; leaf tissues

613 from four different transgenic plants). Student's *t*-tests were performed for data (mean ±

29

614 standard deviation) and P-values are indicated (asterisks). *DCL2i* does not affect

615 expression of *DCL1*, *DCL3* or *DCL4* (A). However *DCL3i* (B) or *DCL4i* (C) resulted in

616 increased mRNA levels of *DCL2*.

617

618 **Figure 3. Distribution of 20-25nt vsiRNAs and siRNA$_{TcvGFP}$ across the**

619 **TCV/GFPΔCP RNA.** (A) *Gfp*. (B) *GfpDCL1i*. (C) *GfpDCL2Ai*. (D) *GfpDCL3Bi*. (E)

620 *GfpDCL4Ai*. The sRNA libraries were generated from sRNA samples extracted from

621 TCV/GFPΔCP-inoculated leaves. Blue and red bars represent siRNAs aligned to the

622 sense (positive) and antisense (negative) strands of TCV/GFPΔCP viral RNA and

623 *TcvGFP* mRNA (highlighted), respectively. The TCV/GFPΔCP genome organisation is

624 indicated.

625

626 **Figure 4. Distribution of 20-25nt *GFP* siRNAs across the 714nt *TcvGFP* mRNA.** (A)

627 *Gfp*. (B) *GfpDCL1i*. (C) *GfpDCL2Ai*. (D) *GfpDCL3Bi*. (E) *GfpDCL4Ai*. The sRNA

628 libraries were generated from sRNA samples extracted from TCV/GFPΔCP-inoculated

629 leaves. Blue and red bars represent siRNAs aligned to the sense (positive) and antisense

630 (negative) strands of *TcvGFP* mRNA, respectively. The two regions (Region 1 and

631 Region 2) having less sequence similarity with that of the transgene *16cGFP* mRNA (see

632 Fig. 5) as well as nucleotide coordinates are indicated.

633

634 **Figure 5. Distribution of 20-25nt *GFP* siRNAs across the 792nt Transgene *16cGFP***

635 **mRNA.** (A) *Gfp*. (B) *GfpDCL1i*. (C) *GfpDCL2Ai*. (D) *GfpDCL3Bi*. (E) *GfpDCL4Ai*. The

636 sRNA libraries were generated from sRNA samples extracted from TCV/GFPΔCP-

637 inoculated leaves. Blue and red bars represent siRNAs aligned to the sense (positive) and

638 antisense (negative) strands of *16cGFP* mRNA, respectively. The two regions (Region 1

639 and Region 2) having less sequence similarity with that of the transgene *TcvGFP* mRNA

640 (see Fig. 4) as well as nucleotide coordinates are indicated.

641

642 **Figure 6. Size Profiles of Transgene *GFP* siRNA$_{16cGFP}$.** (A) *Gfp*. (B) *GfpDCL1i*. (C)

643 *GfpDCL2Ai*. (D) *GfpDCL3Bi*. (E) *GfpDCL4Ai*. The sRNA libraries were generated from

644 sRNA samples extracted from leaves with mock (left) or TCV/GFPΔCP (right)

645   inoculation. Blue and red bars represent siRNAs aligned to the sense and antisense

646   strands of the transgene *16cGFP* mRNA respectively.

647

648   **Figure 7. Size Profiles of TCV/GFPΔCP Viral siRNAs.** (A) *Gfp*. (B) *GfpDCL1i*. (C)

649   *GfpDCL2Ai*. (D) *GfpDCL3Bi*. (E) *GfpDCL4Ai*. The sRNA libraries were generated from

650   sRNA samples extracted from leaves with mock (left) or TCV/GFPΔCP (right)

651   inoculation. Blue and red bars represent siRNAs aligned to the sense and antisense

652   strands of TCV/GFPΔCP RNA, respectively.

653

654   **Figure 8. Cell- and Non-cell Autonomous VIGS in *N. benthamiana*.** In incipient leaf

655   epidermal cells (*i.e.* individual cells initially infected by TCV/GFPΔCP), *DCL4* plays a

656   critical role in biogenesis of vsiRNAs, siRNA$_{TCVGFP}$ and transgene siRNA$_{16cGFP}$. These

657   siRNAs are associated with cell-autonomous intracellular VIGS (Intra-VIGS) to inhibit

658   local virus infection. DCL4-processed siRNAs are unlikely involved in spread of VIGS

659   from leaf epidermal cell to adjacent cells because *DCL4* inhibits intercellular VIGS. In

660   the incipient cell, *DCL2* can also target and dice viral RNAs, *TcvGFP* and *16cGFP*

661   mRNA into siRNAs, but this activity is largely blocked by *DCL4* (**T** sign). In contrast,

662   the key functionality of *DCL2* is to trigger efficient intercellular VIGS (Inter-VIGS). This

663   is likely achieved through its activities to produce DCL2-processed/dependent siRNAs

664   (and/or their precursor long RNAs, highlighted red) in incipient cells and to perceive

665   these mobile signals for non-cell autonomous inter-VIGS in recipient epidermal and

666   mesophyll cells. Neither *DCL1* nor *DCL3* affects vsiRNA production, intra- and

667   intercellular VIGS. Thus *DCL4* and *DCL2* play major but distinct roles in cell- and non-

668   cell autonomous VIGS that form a dual antiviral frontline in incipient and recipient cells.

669   *DCL4*, the primary defender for the cell-autonomous intracellular VIGS, can attack

670   viruses within the initially infected cells. However, if viruses break through this defence

671   frontline, non-cell autonomous intracellular VIGS can efficiently spread to nearby

672   recipient cells. This is due to loss of the negative control of intercellular VIGS mediated

673   by *DCL4*. Intercellular VIGS is dependent upon functional *DCL2* and DCL2-

674   processed/dependent siRNAs (and/or their precursor long RNAs), but it is negatively

675   controlled by *DCL4*. RNAi of *DCL4* results in fully functional *DCL2* that enhances cell-

676   to-cell spread of VIGS. The intercellular VIGS can then defend recipient cells from

677   further virus infection. Such a dual-defence strategy can compensate each other to give

678   host cells evolutionary advantage to battle against virus infection. This model is relevant

679   to virus-VIGS interaction at the intra-/intercellular level, rather than to systemic virus

680   infection. The potential spread of DCL2-processed/dependent siRNAs (and their

681   precursor long RNAs, highlighted red) to move from the incipient to recipient cell

682   through plasmodesmata is indicated with dashed arrows and cylinder signs.

683

684

Parsed Citations

Aliyari, R. and Ding, S.W. (2009). RNA-based viral immunity initiated by the Dicer family of host immune receptors. Immunol. Rev. 227: 176-188.
Pubmed: Author and Title
CrossRef: Author and Title
Google Scholar: Author Only Title Only Author and Title

Andika, I.B., Maruyama, K., Sun, L., Kondo, H., Tamada, T., and Suzuki, N. (2015). Differential contributions of plant Dicer-like proteins to antiviral defences against potato virus X in leaves and roots. Plant J. 81: 781-793.
Pubmed: Author and Title
CrossRef: Author and Title
Google Scholar: Author Only Title Only Author and Title

Aregger, M., Borah, B.K., Seguin, J., Rajeswaran, R., Gubaeva, E.G., Zvereva, A.S., Windels, D., Vazquez, F., Blevins, T., Farinelli, L., et al., (2012). Primary and secondary siRNAs in geminivirus-induced gene silencing. PLoS Pathog. 8: e1002941.
Pubmed: Author and Title
CrossRef: Author and Title
Google Scholar: Author Only Title Only Author and Title

Baulcombe, D. (2004). RNA silencing in plants. Nature 431: 356-363.
Pubmed: Author and Title
CrossRef: Author and Title
Google Scholar: Author Only Title Only Author and Title

Berg, J.M. (2016) Retraction. Science 354: 190.
Pubmed: Author and Title
CrossRef: Author and Title
Google Scholar: Author Only Title Only Author and Title

Blevins, T., Rajeswaran, R., Shivaprasad, P.V., Beknazariants, D., Si-Ammour, A, Park, H.S., Vazquez, F., Robertson, D., Meins, F. Jr., Hohn, T., et al. (2006). Four plant Dicers mediate viral small RNA biogenesis and DNA virus induced silencing. Nucleic Acids Res. 34: 6233-6246.
Pubmed: Author and Title
CrossRef: Author and Title
Google Scholar: Author Only Title Only Author and Title

Bouche, N., Lauressergues, D., Gasciolli, V., and Vaucheret, H. (2006).An antagonistic function for Arabidopsis DCL2 in development and a new function for DCL4 in generating viral siRNAs. EMBO J. 25: 3347-3356.
Pubmed: Author and Title
CrossRef: Author and Title
Google Scholar: Author Only Title Only Author and Title

Carrington, J.C., Heaton, L.A, Zuidema, D., Hillman, B.I., and Morris, T.J. (1989). The genome structure of turnip crinkle virus. Virology 170: 219-26.
Pubmed: Author and Title
CrossRef: Author and Title
Google Scholar: Author Only Title Only Author and Title

Chattopadhyay, M., Stupina, V.A, Gao, F., Szarko, C.R., Kuhlmann, M.M., Yuan, X., Shi, K., and Simon, A.E. (2015). Requirement for host RNA-silencing components and the virus-silencing suppressor when second-site mutations compensate for structural defects in the 3' untranslated region. J. Virol. 89: 11603-11618.
Pubmed: Author and Title
CrossRef: Author and Title
Google Scholar: Author Only Title Only Author and Title

Chen, H.M., Chen, L.T., Patel, K., Li, Y.H., Baulcombe, D.C., and Wu, S.H. (2010).22-nucleotide RNAs trigger secondary siRNA biogenesis in plants. Proc. Natl. Acad. Sci. USA 107: 15269-15274 (2010).
Pubmed: Author and Title
CrossRef: Author and Title
Google Scholar: Author Only Title Only Author and Title

Cohen, Y., Gisel, A, and Zambryski, P.C. (2000). Cell-to-cell and systemic movement of recombinant green fluorescent protein-tagged turnip crinkle viruses. Virology 273: 258-266
Pubmed: Author and Title
CrossRef: Author and Title
Google Scholar: Author Only Title Only Author and Title

Csorba, T., Kontra, L., and Burgyan, J. (2015). Viral silencing suppressors: Tools forged to fine-tune host-pathogen coexistence. Virology 479-480: 85-103.
Pubmed: Author and Title
CrossRef: Author and Title
Google Scholar: Author Only Title Only Author and Title

Dunoyer, P., Himber, C., and Voinnet, O. (2005). DICER-LIKE 4 is required for RNA interference and produces the 21-nucleotide small interfering RNA component of the plant cell-to-cell silencing signal. Nat. Genet. 37: 1356-1360.
Pubmed: Author and Title
CrossRef: Author and Title
Google Scholar: Author Only Title Only Author and Title

Fusaro, A.F., Matthew, L., Smith, N.A, Curtin, S.J., Dedic-Hagan, J., Ellacott, G.A, Watson, J.M, Wang, M.B., Brosnan, C., Carroll, B.J., et al. (2006). RNA interference-inducing hairpin RNAs in plants act through the viral defence pathway. EMBO Rep. 7: 1168-1175.
Pubmed: Author and Title
CrossRef: Author and Title
Google Scholar: Author Only Title Only Author and Title

Garcia-Ruiz, H., Takeda, A, Chapman, E.J., Sullivan, C.M., Fahlgren. N., Brempelis, K.J., and Carrington, J.C. (2010). Arabidopsis RNA-dependent RNA polymerases and Dicer-like proteins in antiviral defense and small interfering RNA biogenesis during Turnip mosaic virus infection. Plant Cell 22: 481-496.
Pubmed: Author and Title
CrossRef: Author and Title
Google Scholar: Author Only Title Only Author and Title

Hacker, D.L., Petty, I.T., Wei, N., and Morris, T.J. (1992). Turnip crinkle virus genes required for RNA replication and virus movement. Virology 186: 1-8.
Pubmed: Author and Title
CrossRef: Author and Title
Google Scholar: Author Only Title Only Author and Title

Hamilton, A.J., and Baulcombe, D.C. (1999). A species of small antisense RNA in posttranscriptional gene silencing in plants. Science 286: 950-952.
Pubmed: Author and Title
CrossRef: Author and Title
Google Scholar: Author Only Title Only Author and Title

Haseloff, J., Siemering, K.R., Prasher, D.C., and Hodge, S. (1997). Removal of a cryptic intron and subcellular localization of green fluorescent protein are required to mark transgenic Arabidopsis plants brightly. Proc. Natl. Acad. Sci. USA 94: 2122-2127.
Pubmed: Author and Title
CrossRef: Author and Title
Google Scholar: Author Only Title Only Author and Title

Henderson, I.R., Zhang, X., Lu, C., Johnson, L., Meyers, B.C., Green, P.J., and Jacobsen, S.E. (2006). Dissecting Arabidopsis thaliana DICER function in small RNA processing, gene silencing and DNA methylation patterning. Nat. Genet. 38: 721-725.
Pubmed: Author and Title
CrossRef: Author and Title
Google Scholar: Author Only Title Only Author and Title

Langmead, B., and Salzberg, S. (2012). Fast gapped-read alignment with Bowtie 2. Nat. Methods 9: 357-359.
Pubmed: Author and Title
CrossRef: Author and Title
Google Scholar: Author Only Title Only Author and Title

Katsarou, K., Mavrothalassiti, E., Dermauw, W., Van Leeuwen, T., and Kalantidis, K. (2016) Combined Activity of DCL2 and DCL3 Is Crucial in the Defense against Potato Spindle Tuber Viroid. PLoS Pathog. 12: e1005936.
Pubmed: Author and Title
CrossRef: Author and Title
Google Scholar: Author Only Title Only Author and Title

Li, C., Zhang, K., Zeng, X., Jackson, S., Zhou, Y., and Hong, Y. (2009). A cis element within flowering locus T mRNA determines its mobility and facilitates trafficking of heterologous viral RNA. J. Virol. 83: 3540-3548.
Pubmed: Author and Title
CrossRef: Author and Title
Google Scholar: Author Only Title Only Author and Title

Li, W. Z., Qu, F., and Morris, T. J. (1998). Cell-to-cell movement of turnip crinkle virus is controlled by two small open reading frames that function in trans. Virology 244: 405-416.
Pubmed: Author and Title
CrossRef: Author and Title
Google Scholar: Author Only Title Only Author and Title

Melnyk, C.W., Molnar, A, and Baulcombe, D.C. (2011). Intercellular and systemic movement of RNA silencing. EMBO J. 30: 3553-3563.
Pubmed: Author and Title
CrossRef: Author and Title
Google Scholar: Author Only Title Only Author and Title

Merai, Z, Kerenyi, Z, Kertesz, S., Magna, M., Lakatos, L., and Silhavy, D. (2006). Double-stranded RNA binding may be a general plant RNA viral strategy to suppress RNA silencing. J. Virol. 80: 5747-5756.
Pubmed: Author and Title
CrossRef: Author and Title
Google Scholar: Author Only Title Only Author and Title

Mlotshwa, S., Pruss, G.J., Peragine, A, Endres, M.W., Li, J., Chen, X., Poethig, R.S., Bowman, L.H., and Vance, V. (2008). DICER-LIKE2 plays a primary role in transitive silencing of transgenes in Arabidopsis. PLoS One 3: e1755.
Pubmed: Author and Title
CrossRef: Author and Title
Google Scholar: Author Only Title Only Author and Title

Mukherjee, K., Campos, H., and Kolaczkowski, B. (2013). Evolution of animal and plant dicers: early parallel duplications and

recurrent adaptation of antiviral RNA binding in plants. Mol. Biol. Evol. 30: 627-641.
Pubmed: Author and Title
CrossRef: Author and Title
Google Scholar: Author Only Title Only Author and Title

Nakasugi, K., Crowhurst, R., Bally, J., and Waterhouse, P. (2014). Combining transcriptome assembly from multiple De novo assemblers in the allo-tetraploid plant Nicotiana benthamiana. PLoS One 9: e91776.
Pubmed: Author and Title
CrossRef: Author and Title
Google Scholar: Author Only Title Only Author and Title

Nakasugi, K., Crowhurst, R.N., Bally, J., Wood, C.C., Hellens, R.P., and Waterhouse, P.M. (2013). De novo transcriptome sequence assembly and analysis of RNA silencing genes of Nicotiana benthamiana. PLoS One 8: e59534.
Pubmed: Author and Title
CrossRef: Author and Title
Google Scholar: Author Only Title Only Author and Title

Pandey, S.P., Shahi, P., Gase, K., and Baldwin, I.T. (2008). Herbivory-induced changes in the small-RNA transcriptome and phytohormone signaling in Nicotiana attenuate. Proc. Natl. Acad. Sci. USA 105: 4559-4564.
Pubmed: Author and Title
CrossRef: Author and Title
Google Scholar: Author Only Title Only Author and Title

Parent, J-S., Bouteiller, N., Elmayan, T., and Vaucheret, H. (2015). Respective contribution of Arabidopsis DCL2 and DCL4 to RNA silencing. Plant J. 81: 223-232.
Pubmed: Author and Title
CrossRef: Author and Title
Google Scholar: Author Only Title Only Author and Title

Perez-Canamas, M., and Hernandez, C. (2015). Key importance of small RNA binding for the activity of a glycine-tryptophan (GW) motif-containing viral suppressor of RNA silencing. J. Biol. Chem. 290: 3106-3120.
Pubmed: Author and Title
CrossRef: Author and Title
Google Scholar: Author Only Title Only Author and Title

Qin, C., Shi, N., Gu, M., Zhang, H., Li, B., Shen, J., Mohammed, A, Ryabov, E., Li, C., Wang, H., et al. (2012). Involvement of RDR6 in short-range intercellular RNA silencing in Nicotiana benthimiana. Sci. Rep. 2: 467.
Pubmed: Author and Title
CrossRef: Author and Title
Google Scholar: Author Only Title Only Author and Title

Qu, F., Ren, T., and Morris, T. J. (2003).The coat protein of turnip crinkle virus suppresses posttranscriptional gene silencing at an early initiation step. J. Virol. 77: 511-522.
Pubmed: Author and Title
CrossRef: Author and Title
Google Scholar: Author Only Title Only Author and Title

Qu, F., Ye, X., and Morris, T.J. (2008). Arabidopsis DRB4, AGO1, AGO7, and RDR6 participate in a DCL4-initiated antiviral RNA silencing pathway negatively regulated by DCL1. Proc. Natl. Acad. Sci. USA 105: 14732-14737.
Pubmed: Author and Title
CrossRef: Author and Title
Google Scholar: Author Only Title Only Author and Title

Qu, J., Ye, J., and Fang, R. (2007). Artificial microRNA-mediated virus resistance in plants. J. Virol. 81: 6690-6699.
Pubmed: Author and Title
CrossRef: Author and Title
Google Scholar: Author Only Title Only Author and Title

Ryabov, E.V., van Wezel. R., Walsh, J., and Hong, Y. (2004). Cell-to-Cell, but not long-distance, spread of RNA silencing that is induced in individual epidermal cells. J. Virol. 78: 3149-3154.
Pubmed: Author and Title
CrossRef: Author and Title
Google Scholar: Author Only Title Only Author and Title

Ryabov, E.V., Wood, G.R., Fannon, J.M., Moore, J.D., Bull, J.C., Chandler, D., Mead, A, Burroughs, N., and Evans D.J. (2014). A virulent strain of Deformed Wing Virus (DWV) of Honeybees (Apis mellifera) prevails after Varroa destructor-mediated, or in vitro, transmission. PLoS Pathog. 10: e1004230.
Pubmed: Author and Title
CrossRef: Author and Title
Google Scholar: Author Only Title Only Author and Title

Ruiz, M.T., Voinnet, O., and Baulcombe, D.C. (1998). Initiation and maintenance of virus-induced gene silencing. Plant Cell 10: 937-946.
Pubmed: Author and Title
CrossRef: Author and Title
Google Scholar: Author Only Title Only Author and Title

Sarkies, P., and Miska, E.A. (2014). Small RNAs break out: the molecular cell biology of mobile small RNAs. Nat. Rev. Mol. Cell Biol. 15: 525-535.
Pubmed: Author and Title

Schwach, F., Vaistij, F.E., Jones, L., and Baulcombe, D.C. (2005). An RNA-dependent RNA polymerase prevents meristem invasion by potato virus X and is required for the activity but not the production of a systemic silencing signal. Plant Physiol. 138: 1842-1852.

Searle, I.R., Pontes, O., Melnyk, C.W., Smith, L.M., and Baulcombe, D.C. (2010). JMJ14, a JmjC domain protein, is required for RNA silencing and cell-to-cell movement of an RNA silencing signal in Arabidopsis. Genes Dev. 24: 986-991.

Shi, Y., Ryabov, E.V., van Wezel, R., Li, C., Jin, M., Wang, W., Fan, Z., and Hong, Y. (2009). Suppression of local RNA silencing is not sufficient to promote cell-to-cell movement of Turnip crinkle virus in Nicotiana benthamiana. Plant Signal Behav. 4: 15-22.

Smith, L.M., Pontes, O., Searle, I., Yelina, N., Yousafzai, F.K., Herr, A.J., Pikaard, C.S., and Baulcombe, D.C. (2007). An SNF2 protein assoicated with nuclear RNA silencing and the spread of a silencing signal between cells in Arabidopsis. Plant Cell 19: 1507-1521.

Thomas, C.L., Leh, V., Lederer, C., and Maule, A.J. (2003). Turnip crinkle virus coat protein mediates suppression of RNA silencing in Nicotiana benthamiana. Virology 306: 33-41.

Wang, X.B., Jovel, J., Udomporn, P., Wang, Y., Wu, Q., Li, W.X., Gasciolli, V., Vaucheret, H., and Ding, S.W. (2011).The 21-nucleotide, but not 22-nucleotide, viral secondary small interfering RNAs direct potent antiviral defence by two cooperative argonautes in Arabidopsis thaliana. Plant Cell 23: 1625-1638.

Xie, Z, Allen, E., Wilken, A, and Carrington, J.C. (2005). DICER-LIKE 4 functions in trans-acting small interfering RNA biogenesis and vegetative phase change in Arabidopsis thaliana. Proc. Natl. Acad. Sci. USA 102: 12984-12989.

Xie, Z, Johansen, L.K., Gustafson, A.M., Kasschau, K.D., Lellis, A.D., Zilberman, D., Jacobsen, S.E., and Carrington, J.C. (2004). Genetic and functional diversification of small RNA pathways in plants. PLoS Biol. 2: E104.

Zhang, X., Singh, J., Li, D., and Qu, F. (2012). Temperature-dependent survival of Turnip crinkle virus-infected Arabidopsis plants relies on an RNA silencing-based defense that requires dcl2, AGO2, and HEN1. J. Virol. 86: 6847-6854.

Zhou, Y., Ryabov, E., Zhang, X., and Hong, Y. (2008). Influence of viral genes on the cell-to-cell spread of RNA silencing. J. Exp. Bot. 59: 2803-2813.